



## Resonance response analysis of nonlinear vibration energy harvesting system under bounded noise excitation



Di Liu, Qianqian Fu

*School of Mathematical Sciences, Shanxi University, Taiyuan, 030006, PR China.*

### Abstract

In this paper, the resonance response of piezoelectric vibration energy harvester (VEH) driven by bounded noise is discussed through the quasi-conservative stochastic averaging method. A nonlinear transformation based on the total energy is firstly established to transform piezoelectric VEH system from an electromechanical coupled nonlinear system into a single-degree-of-freedom (SDOF) system. Then the SDOF system is rewritten as Itô stochastic system about the energy and residual phase under the case of  $p:q$  resonance through the quasi-conservative stochastic averaging method. And the joint probability density function (JPDF) of the stationary response is obtained by solving the corresponding two-dimensional Fokker-Planck-Kolmogorov (FPK) equation using the finite difference method. Meanwhile, the mean-square electric voltage and the mean output power are further analytically given through the JPDF. Finally, the resonance response of piezoelectric VEH system is analyzed in detail in case of the primary resonance, and the Monte Carlo (MC) simulation technique is adopted to validate the effectiveness of the finite difference method.

**Keywords:** Nonlinear vibration energy harvesting, resonance response, bounded noise, quasi-conservative stochastic averaging method, finite difference method.

**2020 MSC:** 70L05, 34C15, 34C29.

©2022 All rights reserved.

### 1. Introduction

With the development of wireless technology, the portable devices, wireless sensors and other MEMS devices have been used more and more widely [19, 23]. However, as a traditional power supply equipment, the battery has some disadvantages including bulky volume, limited lifetime and frequent replacement, etc. All of these can add the difficulty of further application of the MEMS devices, especially in complex geology condition. As an effective way to get clean energy, the vibration energy harvester (VEH) is capable of generating electricity spontaneously and can transform vibration mechanical energy of the environment into electrical energy, which provides power to low-power MEMS devices and has gained more and more attention.

In general, the energy harvesting mechanisms of VEH devices include electrostatic, electromagnetic and piezoelectric. And the piezoelectric transduction mechanism has prominent mechanical energy harvesting mechanism owing to its high electromechanical coupling coefficient and piezoelectric coefficient

Email addresses: [di-lau@hotmail.com](mailto:di-lau@hotmail.com) (Di Liu), [13015401873@163.com](mailto:13015401873@163.com) (Qianqian Fu)

doi: [10.22436/jnsa.015.01.01](https://doi.org/10.22436/jnsa.015.01.01)

Received: 2021-03-26 Revised: 2021-04-16 Accepted: 2021-04-26

and has been widely studied and applied. In addition, the VEH systems can also be classified into linear and nonlinear system according to the structures of dynamics. Compared with the linear structure, the nonlinear structure can progressively extend the frequency response range and energy collection efficiency of VEH system, and even implement large periodic motion under the excitation of low frequency and low amplitude [6, 25]. As research continues, there are many different nonlinear VEH systems that have been designed and studied through constructing nonlinear oscillation characteristic, such as monostable [12, 30], bistable [24, 34] and tristable states [13, 32, 33], etc. For example, Yang et al. [27, 28] concluded that the high-efficiency compressive-mode piezoelectric VEH can cause high power output with wide working bandwidth and has favorable nonlinear phenomena at low frequency range. Then the monostable piezoelectric VEH under low-level excitation was presented and it could be found that the system can exhibit rich dynamic features, including the softening hysteresis, tunable operating bandwidth, and adjustable voltage and power levels [4]. Lopes et al. [18] investigated the bistable piezo-magneto-elastic VEH to determine the influence of parameters of external force on the system response, such as time series, phase space trajectories, Poincare maps and bifurcation diagrams. And the harmonic balance method was developed to study the nonlinear tristable VEH and it is feasible to achieve the high energy interwell oscillation in the multi-solution range of the tristable VEH [31]. Panyam et al. [20] researched the effective bandwidth of tristable VEH which decreases with the increase of the electromechanical coupling result.

It is well known that the noises are widely existing in various systems of the natural world, and there is a great deal of researches indicating that the noises play an important role in influencing the dynamics of the system, especially nonlinear system, so the VEH techniques based on the noise have gotten increasing interest in recent years. For example, Jiang et al. [10] used the state-space-split method to investigate the statistical characteristics of strongly nonlinear VEH with Gaussian white noise excitation. Ramakrishnan et al. [21] researched the stochastic stability of the piezoelectric VEH under parametric excitation. The stochastic responses of nonlinear piezoelectric VEH under Gaussian colored noise and filtered Gaussian white noise were discussed, respectively [14, 15]. In particular, the bounded noise [3, 9, 16, 17, 26, 29], which can induce resonance has been considered as a reasonable noise model, because it has Dryden spectrum and Von Kaman spectrum in atmospheric turbulence, wind turbulence and seismic ground motion. Zhu et al. [8, 35] researched the resonance response and optimal feedback control of strongly non-linear system with bounded noise when the  $p/q$  resonance happened. Besides, another stochastic analysis method, namely the multiple scales method was proposed to study the dynamical behaviour of the Duffing system subject to the bounded noise [22]. Subsequently, the stochastic averaging method was further expanded to discuss the stochastic response characters of the strongly non-linear oscillator under bounded noise excitation with fractional derivative damping [7] and time-delayed feedback [5], respectively. Recently, Bobryk [2] found that the stochastic multiresonance can be induced when a harmonic oscillator has parametric bounded noise and external periodic force. Precisely because the bounded force has made so plentiful dynamics phenomena, particularly the resonant frequencies which can cause greater amplitude than other frequencies, the impact of bounded force on the capture efficiency of VEH system attract more and more public attention. For example, Alevras [1] researched the optimal condition for stochastic resonance of VEH system with harmonic force and Gaussian white noise, and explored the effect of realistic architecture in the electrical circuit on the achievable power output and the system dynamics. Jin et al. [11] developed the multiple scales method to analyze the dynamics of the bistable VEH system of the time-delayed feedback circuit under narrow-band random process. However, to the best knowledge of authors, no attention has been paid to the resonant response of nonlinear resonance vibration energy harvester (RVEH). To compensate the lack of research, in this manuscript we will focus on the study of the resonant response of nonlinear VEH subject to the bounded noise excitation.

The paper is organized as follows. Sect. 2 gives the mathematical model of the nonlinear RVEH system under bounded noise and introduces a transformation to uncoupled to get a single-degree-of-freedom (SDOF) system. Sect. 3 derives the analytical expression of the joint probability density function (JPDF) and the mean-square electric voltage by the  $p/q$  resonance and the stochastic averaging method. Sect. 4 gives an example of the primary resonance case and studies the effects of the nonlinear stiffness

coefficient, the electromechanical coupling coefficient and the frequency perturbation strength on the random response of RVEH and the mean-square electric voltage. Finally, some concluding remarks are made in Sect. 5.

## 2. Mathematical modelling

Considering a class of nonlinear resonance vibration energy harvester (RVEH) with piezoelectric work mechanism subject to the bounded noise excitation, and the corresponding dimensionless equation of motion can be written as

$$\ddot{X} + c\dot{X} + \omega_0^2 X + \alpha X^3 + \beta V = \xi(t), \quad (2.1)$$

$$\dot{V} + \lambda V = \dot{X}, \quad (2.2)$$

where  $X$  means the oscillator displacement and the dot is the differentiation with respect to  $t$ ;  $c$  represents the linear viscous damping coefficient;  $\omega_0^2$  and  $\alpha$  denote the linear and cubic nonlinear stiffness coefficient;  $\beta$  is the electromechanical coupling coefficient;  $V$  is the output voltage;  $\xi(t)$  stands for a bounded noise and it can be described as

$$\xi(t) = f \cos(\Omega t + \sigma B(t)), \quad (2.3)$$

in which  $f$  is a constant representing the amplitude of the stochastic excitation;  $\Omega$  and  $\sigma^2$  are also constants representing the center frequency and the strength of frequency perturbation, respectively, of the bounded noise;  $B(t)$  stands for a standard Wiener process; and  $\xi(t)$  is a stationary random process in a wide sense with auto correlation function

$$R(\tau) = \frac{f^2}{2} \exp\left(-\frac{\sigma^2}{2} |\tau|\right) \cos \Omega \tau$$

and spectral density

$$S(\omega) = \frac{f^2 \sigma^2}{4\pi} \frac{\omega^2 + \Omega^2 + \frac{1}{4}\sigma^4}{(\omega^2 - \Omega^2 - \frac{1}{4}\sigma^4)^2 + \sigma^4 \omega^2}.$$

Obviously the bandwidth of process  $\xi(t)$  depends mainly on the parameter  $\sigma$ , and it becomes a narrow-band process when  $\sigma$  is small, or is a wide-band process.

For the undamped free vibration system corresponding to system (2.1)-(2.2), we introduce a transformation

$$\text{sgn} X \sqrt{U(X)} = \sqrt{H} \cos \theta, \quad (2.4)$$

$$\dot{X} = -\sqrt{2H} \sin \theta, \quad (2.5)$$

where  $U(X)$  and  $H$  are potential energy and total energy of undamped free motion of system (2.1)-(2.2).  $\theta = \theta(t)$  is the total phase angle and

$$\theta = \theta(t) = \nu(t) + \phi, \quad \frac{d\nu}{dt} = \tilde{\omega}(H, \theta).$$

Here  $\tilde{\omega}(H, \theta)$  represents the instantaneous frequency and  $\phi$  denotes the residual phase angle. Expanding  $\tilde{\omega}^{-1}(H, \theta) = dt/d\nu$  into Fourier series, the following equation can be obtained [8]:

$$\tilde{\omega}^{-1}(H, \theta) = C_0(H) + \sum_{n=1}^{\infty} C_n(H) \cos n\theta, \quad (2.6)$$

in which  $C_i(H)$  ( $i = 0, 1, 2, \dots$ ) are the Fourier coefficients. Then integrating Eq. (2.6) with respect to  $v$ , one can obtain

$$t = C_0(H)v + \sum_{n=1}^{\infty} \frac{1}{n} C_n(H) \sin n\theta. \quad (2.7)$$

Hence the period  $T(H)$  is obtained by integrating Eq. (2.6) from 0 to  $2\pi$  in  $v$ . So

$$T(H) = 2\pi C_0(H)$$

and the average frequency  $\omega(H)$  of the oscillator can be expressed as

$$\omega(H) = \frac{2\pi}{T(H)} = \frac{1}{C_0(H)}.$$

Then

$$\theta(t) \approx \omega(H)t + \phi.$$

Now consider the random vibration of RVEH system (2.1)-(2.2). Then the corresponding variables  $H(t)$  and  $\theta(t)$  of transformation (2.4)-(2.5) are all random processes.  $H(t)$  is slowly varying and  $\phi = \phi(t)$  denotes the residual phase and it is slowly varying. Therefore, one can obtain the following expression

$$\begin{aligned} \theta(t - \tau) &= \omega(H)(t - \tau) + \phi(t - \tau) = \omega(H)(t - \tau) + \phi(t) = \theta(t) - \omega(H)\tau, \\ \dot{X}(t - \tau) &= -\sqrt{2H} \sin(\theta(t - \tau)) = \dot{X} \cos(\omega(H)\tau) + \text{sgn}X \sqrt{2U(X)} \sin(\omega(H)\tau). \end{aligned} \quad (2.8)$$

Integrating the electric equation (2.2), and substituting Eq. (2.8) into the integrated results, the electric voltage might be represented as

$$V \doteq \int_0^t \dot{X}(t - \tau) \exp(-\lambda\tau) d\tau = \frac{\omega^2(H)}{\lambda^2 + \omega^2(H)} X + \frac{\lambda}{\lambda^2 + \omega^2(H)} \dot{X}. \quad (2.9)$$

Substituting expression (2.9) into Eq. (2.1), then the nonlinear coupled RVEH system (2.1)-(2.2) is approximately rewritten as

$$\ddot{X} + (c + C(H))\dot{X} + (\bar{\omega}^2(H) + \omega_0^2)X + \alpha X^3 = f \cos(\Omega t + \sigma B(t)), \quad (2.10)$$

where  $C(H) = \beta\lambda / [\lambda^2 + \omega^2(H)]$  and  $\bar{\omega}^2(H) = \beta\omega^2(H) / [\lambda^2 + \omega^2(H)]$ . Then

$$U(X) = \frac{1}{2} (\bar{\omega}^2(H) + \omega_0^2) X^2 + \frac{1}{4} \alpha X^4, \quad H = \frac{1}{2} \dot{X}^2 + U(X).$$

### 3. Resonance responses

#### 3.1. Stochastic averaging of quasi-conservative

In this study, we aim to analyze the resonance response of VEH system (2.10) through the quasi-conservative stochastic averaging technique. Substituting Eq. (2.4)-(2.5) into Eq. (2.10), the following two

first-order differential equation about  $H(t)$  and  $\phi(t)$  can be obtained:

$$\begin{aligned} \dot{H} &= -2H(c + C(H)) \sin^2 \theta - f\sqrt{2H} \sin \theta \cos(\Omega t + \Lambda) = F_1(H, \theta, \Omega t + \Lambda), \\ \dot{\phi} &= -(c + C(H)) \sin \theta \cos \theta - \frac{f}{\sqrt{2H}} \cos \theta \cos(\Omega t + \Lambda) = F_2(H, \theta, \Omega t + \Lambda), \end{aligned} \tag{3.1}$$

where  $\Lambda = \sigma B(t)$ . In this investigation, the narrow-band excitation and resonant case will be considered when the parameter  $\sigma$  is small, so the following relationship exists

$$\frac{\Omega}{\omega(H)} = \frac{q}{p} + \delta, \tag{3.2}$$

where  $p$  and  $q$  are relatively prime positive small integers and  $\delta$  is a detuning parameter, then applying the Eqs. (2.7) and (3.2), one can obtain

$$\Omega t = \frac{q}{p} \theta(t) + \delta v(t) - \frac{q}{p} \phi(t) + \Omega \sum_{n=1}^{\infty} \frac{1}{n} C_n(H) \sin n\theta.$$

For convenience, we introduce two new variables

$$\Gamma = \delta v(t) - \frac{q}{p} \phi(t) + \Lambda, \quad \Psi = \Psi(H, \theta) = \frac{q}{p} \theta(t) + \Omega \sum_{n=1}^{\infty} \frac{1}{n} C_n(H) \sin n\theta, \tag{3.3}$$

then the variable  $\Omega t + \Lambda$  can be rewritten as

$$\Omega t + \Lambda = \Psi + \Gamma. \tag{3.4}$$

Substituting Eqs. (3.3) and (3.4) into Eq. (3.1), the following Itô stochastic differential equations can be derived:

$$dH = F_1(H, \theta, \Psi + \Gamma) dt, \quad d\Gamma = \left[ \left( \frac{\Omega}{\omega(H)} - \frac{q}{p} \right) \tilde{\omega}(H, \theta) - \frac{q}{p} F_2(H, \theta, \Psi + \Gamma) \right] dt + \sigma dB(t),$$

in which

$$\begin{aligned} F_1(H, \theta, \Psi + \Gamma) &= -2(c + C(H)) H \sin^2 \theta - f\sqrt{2H} \sin \theta \cos(\Psi + \Gamma), \\ F_2(H, \theta, \Psi + \Gamma) &= -(c + C(H)) \sin \theta \cos \theta - \frac{f}{\sqrt{2H}} \cos \theta \cos(\Psi + \Gamma). \end{aligned}$$

$H$  and  $\phi$  are the slowly varying process comparing to  $\theta$ , so  $\Gamma$  is also slowly varying. Furthermore, the total energy process  $H$  and process  $\Gamma$  are approximately Markovian, and the quasi-conservative stochastic averaging technique can be applied and we can obtain the following averaged Itô stochastic differential equation

$$dH = m_1(H, \Gamma) dt, \quad d\Gamma = m_2(H, \Gamma) dt + \sigma dB(t), \tag{3.5}$$

where

$$\begin{aligned} m_1(H, \Gamma) &= -H(c + C(H)) + \sqrt{2H} f \sin \Gamma \langle \sin \theta \sin \Psi \rangle_{\theta}, \\ m_2(H, \Gamma) &= \left( \frac{\Omega}{\omega(H)} - \frac{q}{p} \right) \langle \tilde{\omega}(H, \theta) \rangle_{\theta} + \frac{q}{p} \frac{f}{\sqrt{2H}} \cos \Gamma \langle \cos \theta \cos \Psi \rangle_{\theta}. \end{aligned}$$

### 3.2. The resonance response of the nonlinear VEH system

The corresponding averaged FPK equation of Eq. (3.5) is

$$\frac{\partial p}{\partial t} = -\frac{\partial [m_1 p]}{\partial H} - \frac{\partial [m_2 p]}{\partial \Gamma} + \frac{1}{2}\sigma^2 \frac{\partial^2 p}{\partial \Gamma^2}, \quad (3.6)$$

where  $p = p(H, \Gamma, t | H_0, \Gamma_0, t_0)$  is the transition joint probability density function (JPDF) of  $H$  and  $\Gamma$  with initial condition  $p = \delta(H - H_0) \delta(\Gamma - \Gamma_0)$ . The boundary condition with respect to  $\Gamma$  is periodic, which means that

$$p|_{\Gamma+2n\pi} = p|_{\Gamma}, \quad \frac{\partial p}{\partial t} \Big|_{\Gamma+2n\pi} = \frac{\partial p}{\partial t} \Big|_{\Gamma}.$$

The boundary conditions with respect to  $H$  are

$$p = \text{finite} \quad \text{when} \quad H = 0, \quad p, \frac{\partial p}{\partial t} \rightarrow 0 \quad \text{when} \quad H \rightarrow \infty.$$

The corresponding stationary JPDF of Eq. (3.6) is obtained when  $\frac{\partial p}{\partial t} = 0$ , that is

$$-\frac{\partial [m_1 p]}{\partial H} - \frac{\partial [m_2 p]}{\partial \Gamma} + \frac{1}{2}\sigma^2 \frac{\partial^2 p}{\partial \Gamma^2} = 0. \quad (3.7)$$

Solving Eq. (3.7) by the finite difference method with mesh of  $60 \times 60$ , we can get the stationary JPDF  $p(H, \Gamma)$  of  $H$  and  $\Gamma$ .  $p(H, \Gamma)$  is periodic with respect to  $\Gamma$ , so in this paper, we only consider  $\Gamma \in [-\pi/2, 3\pi/2]$ . The stationary marginal probability density function of the total energy  $H$  is

$$p(H) = \int_{-\pi/2}^{3\pi/2} p(H, \Gamma) d\Gamma.$$

Then, the stationary JPDF of the displacement  $X$  and velocity  $\dot{X}$  can be obtained from

$$p(X, \dot{X}) = \frac{p(H)}{T(H)} \Big|_{H=\frac{1}{2}\dot{X}^2+U(X)}.$$

Naturally, applying the relation between displacement, velocity and electric voltage, which has been given in Eq. (2.9), the mean square value of the electric voltage can be written as

$$\begin{aligned} E(V^2) &= E \left[ \left( \frac{\omega^2(H)}{\lambda^2 + \omega^2(H)} X + \frac{\lambda}{\lambda^2 + \omega^2(H)} \dot{X} \right)^2 \right] \\ &= \int_{-\infty}^{\infty} \int_{-\infty}^{\infty} \left( \frac{\omega^2(H)}{\lambda^2 + \omega^2(H)} X + \frac{\lambda}{\lambda^2 + \omega^2(H)} \dot{X} \right)^2 p(X, \dot{X}) dX d\dot{X}, \end{aligned}$$

and at the same moment the mean output power  $E(P)$  can be further given according to the linear square relationship between the power and the electric voltage:

$$E(P) = \beta \lambda E(V^2).$$

The above special case and their examination allow a further understanding of the generality of the derived equations. Then the next section gives an example to illustrate their uses and advantages.

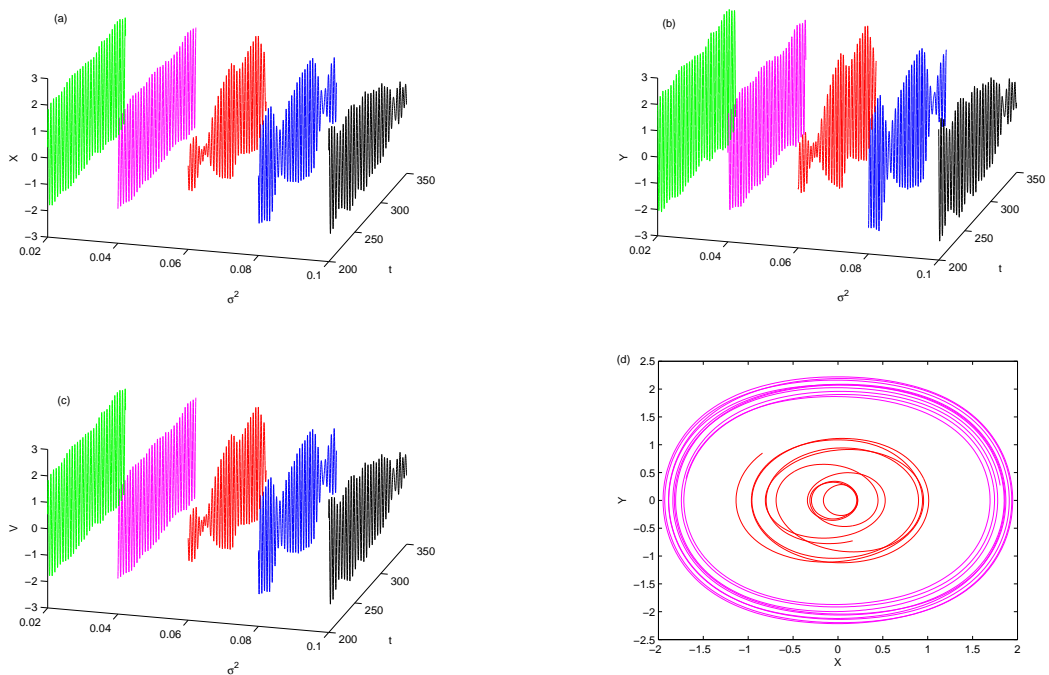


Figure 1: The time history of (a) displacement  $X$ , (b) velocity  $\dot{X}$ , (c) output voltage  $V$  with different frequency perturbation strength, (d) phase space trajectory ( $\alpha = 0.2$ ,  $c = 0.02$ ,  $\omega_0^2 = 0.5$ ,  $\Omega = 1.2$ ,  $f = 0.2$ ,  $\lambda = 0.1$ ,  $\beta = 0.5$ ).

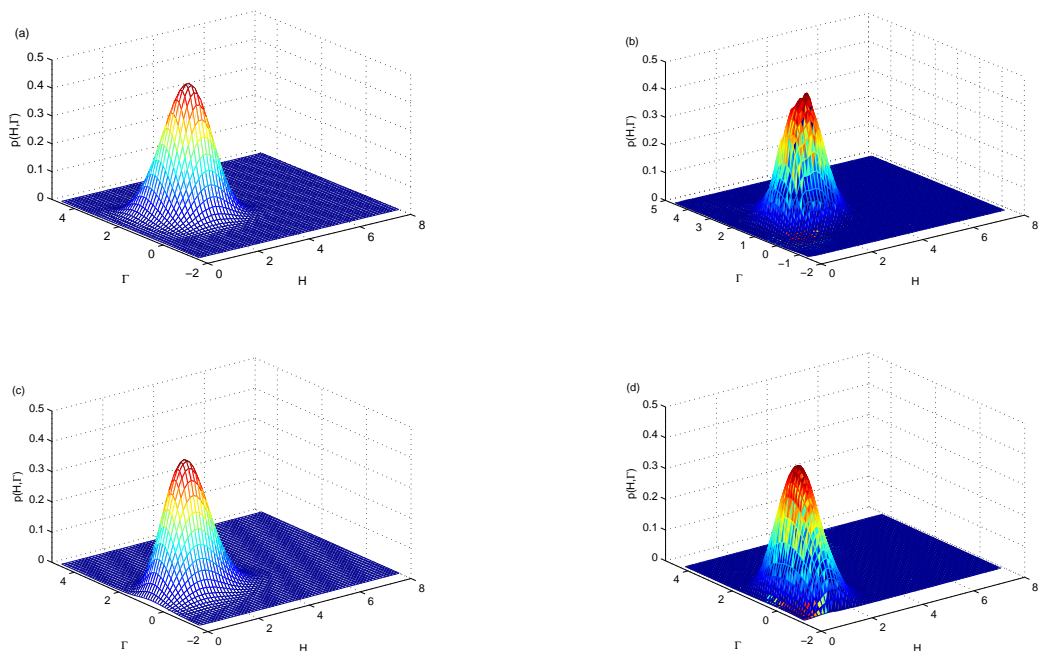


Figure 2: Stationary JPDF  $p(H, \Gamma)$  of system(1),  $c = 0.02$ ,  $\omega_0^2 = 0.5$ ,  $\Omega = 1.2$ ,  $f = 0.2$ ,  $\sigma^2 = 0.02$ ,  $\lambda = 0.1$ ,  $\beta = 0.5$ ,  $p = 1$ ,  $q = 1$ . (a)  $\alpha = 0.2$ , finite difference method; (b)  $\alpha = 0.2$ , MC method; (c)  $\alpha = 0.3$ , finite difference method; (d)  $\alpha = 0.3$ , MC method.

#### 4. Probabilistic analysis of primary resonance response

As an example, the primary resonance case ( $p = q = 1$ ) is used to investigate the effectiveness of the proposed solution procedure. In this case, the effects of various physical parameters on the JPDF of the VEH system are examined, and the changes of the corresponding energy collection efficiency are also analyzed. These physical parameters include the nonlinear stiffness coefficient  $\alpha$ , the electromechanical coupling coefficient  $\beta$  and the frequency perturbation strength  $\sigma^2$ . In Eqs. (2.1)-(2.2) and Eqs. (2.3), the parameters of the stochastic RVEH system are given as  $\alpha = 0.2$ ,  $c = 0.02$ ,  $\omega_0^2 = 0.5$ ,  $\Omega = 1.2$ ,  $f = 0.2$ ,  $\sigma^2 = 0.02$ ,  $\lambda = 0.1$ , and  $\beta = 0.5$ , unless otherwise mentioned.

##### 4.1. Primary resonance response analysis of system

First, the stochastic response of system (2.1)-(2.2) is studied in detail. The time histories and phase space trajectory of system (2.1)-(2.2) subject to different frequency perturbation strengths  $\sigma^2$  are shown in Fig. 1. Notice that in Fig. 1, every color corresponds to a value of  $\sigma^2$ , such as the red represents the case of  $\sigma^2 = 0.06$ . According to the comparison and analysis, we can see that the increase of frequency perturbation strength  $\sigma^2$  exacerbate the response amplitude's volatility, that is a typical random jump phenomenon, which eventually causes the output voltage of RVEH system changes. By the phase space trajectory in Fig. 1(d), it is more closer to the center with the increase of frequency perturbation strengths  $\sigma^2$ . Meanwhile, to verify the effectiveness of the proposed method in Sect. 3, the analysis results of different nonlinear stiffness coefficients  $\alpha$  getting by the finite difference method are given in Figs. 2(a) and 2(c). The Monte Carlo (MC) method is then used to estimate the above results of analysis, which are shown in Figs. 2(b) and 2(d). By comparison, it can be found that the proposed method is a highly effective means for strong nonlinear RVEH system.

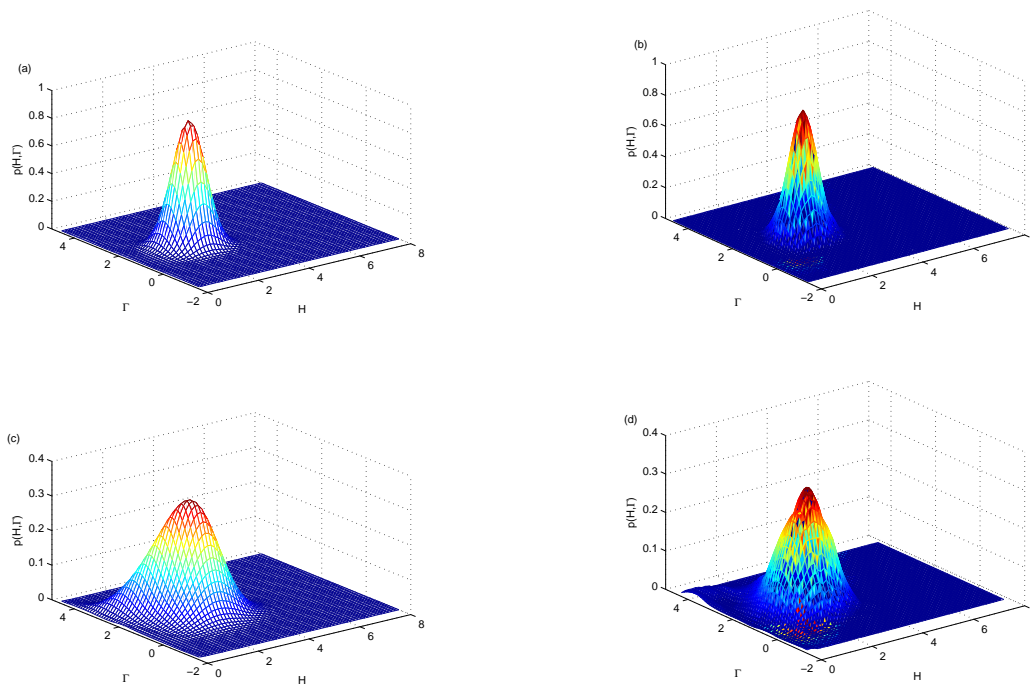


Figure 3: Stationary JPDF  $p(H, \Gamma)$  of system(1),  $\alpha = 0.2$ ,  $c = 0.02$ ,  $\omega_0^2 = 0.5$ ,  $\Omega = 1.2$ ,  $f = 0.2$ ,  $\lambda = 0.1$ ,  $\beta = 0.5$ ,  $p = 1$ ,  $q = 1$ . (a)  $\sigma^2 = 0.01$ , finite difference method; (b)  $\sigma^2 = 0.01$ , MC method; (c)  $\sigma^2 = 0.03$ , finite difference method; (d)  $\sigma^2 = 0.03$ , MC method.

Then the effects of the frequency perturbation strength  $\sigma^2$  upon the JPDF are discussed, which are shown in Figs. 3(a) and 3(c). It shows that the JPDF has a single peak, and the results are given by

proposed procedure. By comparing the changes in the shape of the JPDF, one can see that a larger diffusion area appear for a greater frequency perturbation strength  $\sigma^2$ . The MC method is then used to estimate the above result of analysis, which are shown in Figs. 3(b) and 3(d), and we find a high degree of consensus.

Finally, to research the influence of the electromechanical coupling coefficient  $\beta$  on the stationary JPDF, the JPDF relative to two different electromechanical coupling coefficients  $\beta = 0.4, 0.6$  by analytical approach are given and shown in Figs. 4(a) and 4(c). Therefore, by comparing the changes for JPDF, one can see that the vibration center and the range of vibration of system undergo significant changes, that is the system has higher level of concentration when the parameter  $\beta$  increases. The corresponding simulation verification has also been given in Figs. 4(b) and 4(d) by the MC techniques, and a good coherence is obtained.

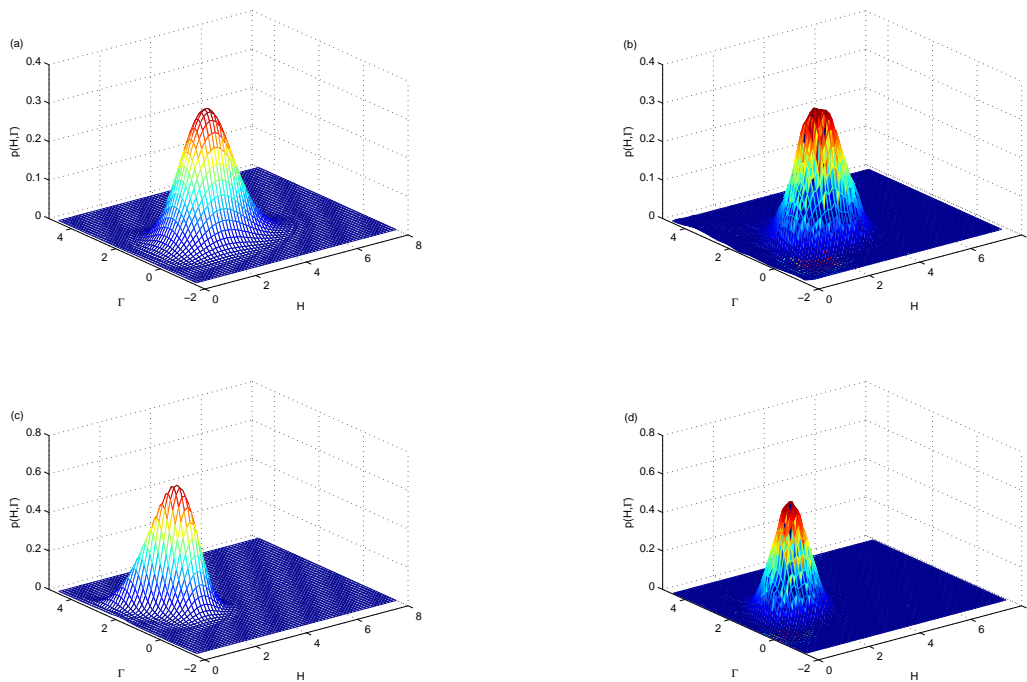


Figure 4: Stationary JPDF  $p(H, \Gamma)$  of system(1),  $\alpha = 0.2, c = 0.02, \omega_0^2 = 0.5, \Omega = 1.2, f = 0.2, \sigma^2 = 0.02, \lambda = 0.1, p = 1, q = 1$ . (a)  $\beta = 0.4$ , finite difference method; (b)  $\beta = 0.4$ , MC method; (c)  $\beta = 0.6$ , finite difference method; (d)  $\beta = 0.6$ , MC method.

#### 4.2. Effects of physical parameters on harvesting performance

The changes of physical parameters of the RVEH cause the stochastic response changes, which further impact on the energy harvesting performance, so the mean square voltage varying with the nonlinear stiffness coefficient  $\alpha$ , the electromechanical coupling coefficient  $\beta$  and the frequency perturbation strength  $\sigma^2$  will be studied in detail in this subsection.

Multiplying  $\dot{X}$  at both sides of Eq. (2.10), we can get

$$\frac{d}{dt} \left[ \frac{1}{2} \dot{X}^2 + \frac{1}{2} \omega_0^2 x^2 + \frac{1}{4} \alpha X^4 \right] + c \dot{X}^2 + (\overline{\omega}^2(H)X + C(H)\dot{X}) \dot{X} = f \dot{X} \cos(\Omega t + \sigma B(t)). \quad (4.1)$$

Note that the right-hand side of Eq. (4.1) is the product of velocity times narrow-band random force, which expresses the instantaneous power. In addition,  $(\overline{\omega}^2(H)X + C(H)\dot{X})\dot{X} = \beta \lambda V^2$  denotes the instantaneous electrical power harvested by the energy harvester. Therefore, the harvested electrical output power

and the mean square voltage are influenced by the nonlinear stiffness coefficient  $\alpha$ , the electromechanical coupling coefficient  $\beta$  and the frequency perturbation intensity  $\sigma^2$ .

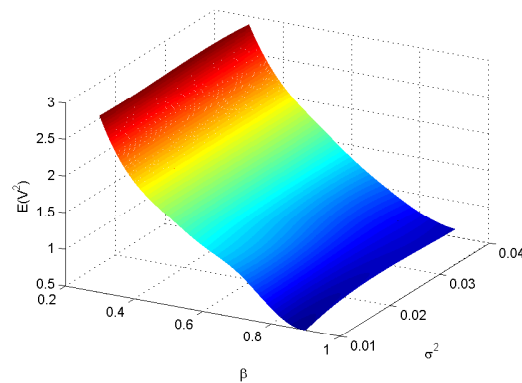


Figure 5: The mean-square electric voltage  $E(V^2)$  on frequency perturbation strength  $\sigma^2$  and electromechanical coupling coefficient  $\beta$ . ( $\alpha = 0.2, c = 0.02, \omega_0^2 = 0.5, \Omega = 1.2, f = 0.2, \lambda = 0.1, p = 1, q = 1$ )

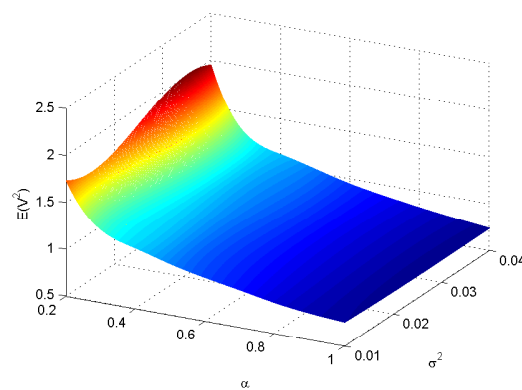


Figure 6: The mean-square electric voltage  $E(V^2)$  on frequency perturbation strength  $\sigma^2$  and nonlinear stiffness coefficient  $\alpha$  ( $c = 0.02, \omega_0^2 = 0.5, \Omega = 1.2, f = 0.2, \lambda = 0.1, \beta = 0.5, p = 1, q = 1$ ).

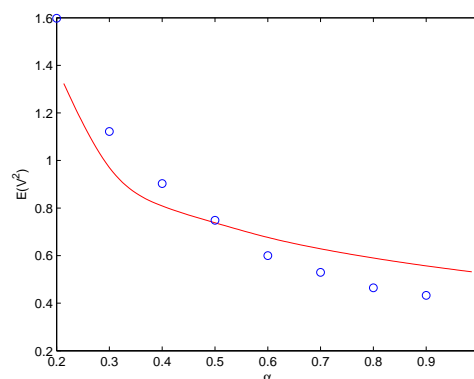


Figure 7: The mean-square electric voltage  $E(V^2)$  on nonlinear stiffness coefficient  $\alpha$  ( $c = 0.02, \omega_0^2 = 0.5, \Omega = 1.2, f = 0.2, \sigma^2 = 0.04, \lambda = 0.1, \beta = 0.5, p = 1, q = 1$ ).

To understand the impact of relevant physical parameters on the energy capture efficiency more

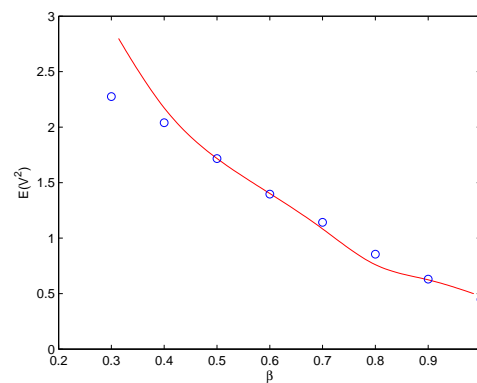


Figure 8: The mean-square electric voltage  $E (V^2)$  on electromechanical coupling coefficient  $\beta$  ( $\alpha = 0.2$ ,  $c = 0.02$ ,  $\omega_0^2 = 0.5$ ,  $\Omega = 1.2$ ,  $f = 0.2$ ,  $\sigma^2 = 0.02$ ,  $\lambda = 0.1$ ,  $p = 1$ ,  $q = 1$ ).

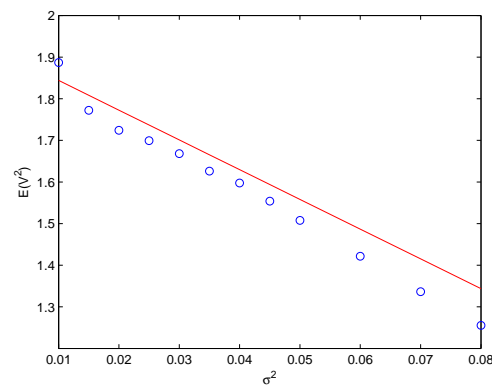


Figure 9: The mean-square electric voltage  $E (V^2)$  on frequency perturbation strength  $\sigma^2$  ( $\alpha = 0.2$ ,  $c = 0.02$ ,  $\omega_0^2 = 0.5$ ,  $\Omega = 1.2$ ,  $f = 0.2$ ,  $\lambda = 0.1$ ,  $\beta = 0.5$ ,  $p = 1$ ,  $q = 1$ ).

clearly, the variation of mean square voltage with frequency perturbation strength  $\sigma^2$  and electromechanical coupling coefficient  $\beta$ , and the variation tendency with frequency perturbation strength  $\sigma^2$  and nonlinear stiffness coefficient  $\alpha$  are given by proposed approach, which are shown in Figs. 5 and 6. It can be seen that the mean-square electric voltage shows the same growth trend as  $\alpha$  and  $\beta$  change, that is the mean-square electric voltage decrease with the increase of these two parameters. By comparing the variation trend, we find that the increase of the electromechanical coupling coefficient  $\beta$  could lead to faster decrease of the mean-square electric voltage than frequency perturbation strength  $\sigma^2$ . In order to verify the effectiveness of the results, the results of MC numerical simulation are used to compare with the theory analysis results, which are shown in Figs. 7 and 8. And the solid lines denote the analytical results by the finite difference method, while the circles represent the results through the MC method. Meanwhile, the effects of  $\sigma^2$  on the mean-square electric voltage are also analyzed for the given  $\alpha$  and  $\beta$  which are shown in Fig. 9, and the trend is also decrease with the increasing of  $\sigma^2$ .

## 5. Conclusions

In this investigation, the quasi-conservative stochastic averaging method is used to analyze the resonance response of the nonlinear VEH system driven by bounded noise excitation. Firstly, a transformation based on total energy of system is introduced to approximate the nonlinear coupled RVEH system into an uncoupled SDOF system. Secondly, under the assumption that the equivalent system is quasi-

conservative, the stochastic averaging method is used to derive the averaged Itô stochastic differential equation about total energy and phase, which are dependent on the ratio of center frequency of bounded noise and the frequency of system. Then the stationary JPFD is obtained through solving the corresponding FPK equation by the finite difference method, and the mean-square electric voltage is also derived through the relation between the electric voltage and the mechanical states. Finally, as an example, we discuss the effects of the nonlinear stiffness coefficient, the electromechanical coupling coefficient and the frequency perturbation strength on the random response of RVEH system in the case of primary resonance. In addition, we also find that these physical parameters have essential effects on the mean-square electric voltage when other parameters unaltered, that is they all lead a reduce of the mean-square electric voltage when these parameters increases, and the corresponding results are verified through direct MC simulation technique.

## Acknowledgment

This work is supported by the National Natural Science Foundations of China under Grant (Nos. 11972019).

## References

- [1] P. Alevras, *On the effect of the electrical load on vibration energy harvesting under stochastic resonance*, ASCE-ASME J. Risk Uncertainty Eng. Syst., Part B: Mech. Eng., **7** (2021), 13 pages. 1
- [2] R. V. Bobryk, *Stochastic multiresonance in oscillators induced by bounded noise-ScienceDirect*, Commun. Nonlinear Sci. Numer. Simul., **93** (2021), 12 pages. 1
- [3] J. Deng, W. C. Xie, M. D. Pandey, *Stochastic stability of a fractional viscoelastic column under bounded noise excitation*, J. Sound Vibr., **333** (2014), 1629–1643. 1
- [4] K. Fan, Q. Tan, Y. Zhang, S. Liu, M. Cai, Y. Zhu, *A monostable piezoelectric energy harvester for broadband low-level excitations*, Appl. Phys. Lett., **112** (2018), 12 pages. 1
- [5] C. S. Feng, R. Liu, *Response of Duffing system with delayed feedback control under bounded noise excitation*, Arch. Appl. Mech., **82** (2012), 1753–1761. 1
- [6] Q. He, M. F. Daqaq, *Electric load optimization of a nonlinear mono-stable duffing harvester excited by white noise*, Meccanica, **51** (2016), 1027–1039. 1
- [7] F. Hu, L. C. Chen, W. Q. Zhu, *Stationary response of strongly non-linear oscillator with fractional derivative damping under bounded noise excitation*, Int. J. Non-Linear Mech., **47** (2012), 1081–1087. 1
- [8] Z. L. Huang, W. Q. Zhu, Y. Q. Ni, J. M. Ko, *Stochastic averaging of strongly non-Linear oscillators under bounded noise excitation*, J. Sound Vibr., **254** (2002), 245–267. 1, 2
- [9] D. Jian, *Higher-order stochastic averaging for a SDOF fractional viscoelastic system under bounded noise excitation*, J. Franklin Inst., **354** (2017), 7917–7945. 1
- [10] W. A. Jiang, P. Sun, Z. W. Xia, *Probabilistic solution of the vibratory energy harvester excited by Gaussian white noise*, Int. J. Dyn. Control, **7** (2019), 167–177. 1
- [11] Y. Jin, Y. Zhang, *Dynamics of a delayed Duffing-type energy harvester under narrow-band random excitation*, Acta Mech., **232** (2021), 1045–1060. 1
- [12] A. Kumar, S. F. Ali, A. Arockiarajan, *Exploring the benefits of an asymmetric monostable potential function in broadband vibration energy harvesting*, Appl. phys. lett., **112** (2018), 23 pages. 1
- [13] H. Li, W. Qin, C. Lan, W. Deng, Z. Zhou, *Dynamics and coherence resonance of tristable energy harvesting system*, Smart Mater. Struct., **25** (2016), 11 pages. 1
- [14] D. Liu, Y. Wu, Y. Xu, J. Li, *Stochastic response of bistable vibration energy harvesting system subject to filtered Gaussian white noise*, Mech. Syst. Signal Process., **130** (2019), 201–212. 1
- [15] D. Liu, Y. Xu, J. Li, *Probabilistic response analysis of nonlinear vibration energy harvesting system driven by Gaussian colored noise*, Chaos Solitons Fractals, **104** (2017), 806–812. 1
- [16] Z. H. Liu, W. Q. Zhu, *Homoclinic bifurcation and chaos in simple pendulum under bounded noise excitation*, Chaos Solitons Fractals, **20** (2004), 593–607. 1
- [17] W. Y. Liu, W. Q. Zhu, Z. L. Huang, *Effect of bounded noise on chaotic motion of duffing oscillator under parametric excitation*, Chaos Solitons Fractals, **12** (2001), 527–537. 1
- [18] V. G. Lopes, J. V. L. L. Peterson, A. Cunha Jr., *Nonlinear characterization of a bistable energy harvester dynamical system*, In: Topics in Nonlinear Mechanics and Physics, **2019** (2019), 71–88. 1
- [19] C. O. Mathuna, T. O'Donnell, R. V. Martinez-Catala, J. Rohan, B. O'Flynn, *Energy scavenging for long-term deployable wireless sensor networks*, Talanta, **75** (2008), 613–623. 1

- [20] M. Panyam, M. F. Daqaq, *Characterizing the effective bandwidth of tri-stable energy harvesters*, J. Sound Vibr., **386** (2017), 336–358. 1
- [21] S. Ramakrishnan, C. Edlund, *Stochastic stability of a piezoelectric vibration energy harvester under a parametric excitation and noise-induced stabilization*, Mech. Syst. Signal Process., **140** (2020), 10 pages. 1
- [22] H. W. Rong, X. D. Wang, G. Meng, W. Xu, T. Fang, *Response of nonlinear oscillator under narrow-band random excitation*, Appl. Math. Mech., **24** (2003), 817–825. 1
- [23] S. Roundy, P. K. Wright, *A piezoelectric vibration based generator for wireless electronics*, Smart Mater. Struct., **13** (2004), 1131–1142. 1
- [24] W. Wang, J. Cao, C. R. Bowen, Y. Zhang, J. Lin, *Nonlinear dynamics and performance enhancement of asymmetric potential bistable energy harvesters*, Nonlinear Dyn., **94** (2018), 1183–1194. 1
- [25] S. Xiao, Y. Jin, *Response analysis of the piezoelectric energy harvester under correlated white noise*, Nonlinear Dyn., **90** (2017), 2069–2082. 1
- [26] X. Yang, W. Xu, Z. Sun, T. Fang, *Effect of bounded noise on chaotic motion of a triple-well potential system*, Chaos Solitons Fractals, **25** (2005), 415–424. 1
- [27] Z. Yang, Y. Zhu, J. Zu, *Theoretical and experimental investigation of a nonlinear compressive-mode energy harvester with high power output under weak excitations*, Smart Mater. Struct., **24** (2015), 025028. 1
- [28] Z. Yang, J. Zu, *High-efficiency compressive-mode energy harvester enhanced by a multi-stage force amplification mechanism*, Energy Conversion and Management, **88** (2014), 829–833. 1
- [29] X. Yue, W. Xu, *Stochastic bifurcation of an asymmetric single-well potential duffing oscillator under bounded noise excitation*, Int. J. Bifurcat. and Chaos, **20** (2010), 3359–3371. 1
- [30] L. Zhao, L. Tang, Y. Yang, *Comparison of modeling methods and parametric study for a piezoelectric wind energy harvester*, Smart Mater. Struct., **22** (2013), 12 pages. 1
- [31] S. Zhou, J. Cao, D. J. Inman, J. Lin, D. Li, *Harmonic balance analysis of nonlinear tristable energy harvesters for performance enhancement*, Journal of Sound and Vibration, **373** (2016), 223–235. 1
- [32] S. Zhou, J. Cao, D. J. Inman, J. Lin, S. Liu, Z. Wang, *Broadband tristable energy harvester: Modeling and experiment verification*, Appl. Energy, **133** (2014), 33–39. 1
- [33] S. Zhou, L. Zuo, *Nonlinear dynamic analysis of asymmetric tristable energy harvesters for enhanced energy harvesting*, Commun. Nonlinear Sci. Numer. Simul., **61** (2018), 271–284. 1
- [34] W. Q. Zhu, G. Q. Cai, R. C. Hu, *Stochastic analysis of dynamical system with double-well potential*, Int. J. Dyn. Control, **1** (2013), 12–19. 1
- [35] W. Q. Zhu, Z. L. Huang, J. M. Ko, Y. Q. NI, *Optimal feedback control of strongly non-linear systems excited by bounded noise*, J. Sound Vibr., **274** (2004), 701–724. 1